Milling parameters and solid waste characterisation to use as supplementary cementitious materials

Parâmetros de moagem e caracterização de resíduos sólidos para aplicação como materiais cimentícios suplementares

Ana Rita Damasceno Costa
Jardel Pereira Gonçalves

Abstract

Despite the increasing number of publications on residual raw materials as supplementary cementitious materials (SCM), the milling beneficiation process and its parameters have been underexplored and presented. In this context, this study aims to evaluate the milling parameters for marble, clay tile, clay brick, and phosphogypsum waste processing for recycling as SCM. The raw materials were benefitted by grinding, sieving, and milling in a planetary ball mill, varying the time and rotation speed parameters. The waste was characterised by helium gas pycnometry, DSC, BET specific surface area, XRF, TGA, and XRD/Rietveld. Waste materials in which the mineral composition of phases was formed at higher temperatures were associated with higher demands for specific milling energy and lower grindability indexes. Marble waste (MW) has a mineral composition similar to commercial limestone and phosphogypsum (PG) can be an alternative to natural gypsum in cementitious materials. Clay brick waste (CBW) and clay tile waste (CTW) have the potential to be used as SCM to replace calcined natural clays, although CTW requires higher energy during milling processes.

Keywords: Milling. Marble waste. Clay tile waste. Clay brick waste. Phosphogypsum. Supplementary cementitious materials.

Resumo

Embora a utilização de matérias-primas residuais como materiais cimentícios suplementares (MCS) seja uma temática crescente na literatura, o processo de beneficiamento por moagem e seus parâmetros ainda são pouco explorados e apresentados. Nesse contexto, o presente estudo visa avaliar os parâmetros de moagem para o beneficiamento dos resíduos de mármore, porcelanato, bloco cerâmico e fosfogesso para reciclagem como MCS. As matérias-primas foram beneficiadas por britagem, peneiramento e moagem em um moinho planetário de bolas variando os parâmetros de tempo e velocidade de rotação. Os resíduos foram caracterizados por picnometria, DSC, área superficial específica BET, FRX, TG e DRX/Rietveld. Os resíduos com composição mineralógica de fases formadas em temperaturas mais elevadas estão associados a maior demanda de energia específica de moagem e menores índices de moabilidade. O RM apresenta composição mineralógica semelhante ao do calcário comercial e o FG pode ser uma alternativa à gipsita natural em materiais cimentícios. O RBC e RP apresentam potencial de uso como MCS em substituição às argilas naturais calcinadas, embora o RP demande maior energia durante o beneficiamento por moagem.

***Palavras-chave**: Moagem. Resíduo de mármore. Resíduo de porcelanato. Resíduo de bloco cerâmico. Fosfogesso. Materiais cimentícios suplementares.*

[1]**Ana Rita Damasceno Costa**
[1]Universidade Federal da Bahia
Salvador - BA - Brasil

[2]**Jardel Pereira Gonçalves**
[2]Universidade Federal da Bahia
Salvador - BA - Brasil

Recebido em 15/11/21
Aceito em 20/04/22

Introduction

Broken ceramic pieces are not accepted as commercial products, and there are no efficient ways to process and recycle this material (LAVAT *et al*., 2009). A study by Pacheco-Torgal and Jalali (2010) showed that the amount of waste generated in the different production stages of the European ceramic industry reaches 3-7% by weight of the total production of red ceramic bricks. It is widely reported that clay brick waste (CBW) can be used as pozzolanic material (SHAO *et al*., 2019; ZHAO *et al*., 2020). When compared to conventional calcined clay, it shows the potential to reduce CO_2 emissions and production costs (TOLEDO FILHO *et al*., 2007). Therefore, CBW has been successfully used as a partial replacement for Portland cement (LASSEUGUETTE *et al*., 2019) as a precursor in alkali-activated binders (ROBAYO-SALAZAR *et al*., 2017) and as a raw material for autoclaved cement production (CONNAN *et al*., 2006).

Brazilian marble production is estimated at 2 million tons per year (CHIODI FILHO, 2018). The solid waste generated during the cutting, shaping, and polishing processes corresponds to almost 25% of the weight of manufactured marble (AYDIN; AREL, 2019). Marble waste (MW) usually consists mainly of calcium carbonate and dolomite, with small fractions of other minerals such as quartz, feldspar, and mica (UYGUNOĞLU *et al*., 2014). Due to its composition, which is often similar to that of limestone, MW is generally used to produce building materials. Various researchers have evaluated its properties when incorporated into cementitious systems (VARDHAN *et al*., 2015; KABEER; VYAS, 2018).

Phosphogypsum (PG) is a waste material from phosphoric acid production in the fertiliser industry and its main chemical composition is $CaSO_4.2H_2O$. It is estimated that Brazil produces approximately 11.6 million tons of PG annually (DEPARTAMENTO…, 2015). Only 15% is reused in different areas (RASHAD, 2017), such as set retarderin the cement industry (SHEN *et al*., 2012). The remaining fraction is disposed of in dumps, resulting in hazardous substance leaching and consequent contamination of groundwater and living beings (CONTRERAS *et al*., 2015).

Although various studies have addressed using waste as an alternative to natural raw materials in cement production, the milling process and its parameters are still underexplored in the literature. It is essential to discuss this because it shows a fundamental analysis of the milling study for residual raw materials. Parameters rarely indicated in the literature are presented and can serve as a guide for future studies that require milling processes. Thus, this study aims to evaluate the milling parameters for marble, clay tile, clay brick, and phosphogypsum waste processing for recycling as SCM. The analysis focuses on the evaluation of milling parameters by identifying the determining variable among the $D_{10\%}$, $D_{50\%}$, $D_{90\%}$ indices, specific surface area, specific milling energy and grindability index. In addition, the second part of the discussion addresses the potential of using this waste as SCM based on the mineralogical composition and content of non-crystalline phases.

Materials and methods

Materials

The raw materials used in this study were phosphogypsum (PG), marble waste (MW), clay brick waste (CBW) and clay tile waste (CTW). The CBW was discarded material from a red ceramic brick factory. The CTW came from a floor covering parts distributor. The sample was from a single batch and model of enamelled clay tile. The MW was Beige Bahia, which was waste obtained from a company that cuts and manufactures ornamental pieces. PG was waste from phosphoric acid production in a fertiliser industry. Samples were collected at several points at the top, bottom, and middle of the dumps. All the collected content was ground and sieved. The sieved fraction of each waste was then quartered to separate batches for milling and storage. The flowchart of the experimental program is shown in Figure 1.

Grinding

The CBW, CTW, and MW consisted of 5-10 cm pieces, which were ground in an I-4198 laboratory jaw crusher (Pavitest). The procedure was performed in two different configurations. Primary grinding with an opening of approximately 30 mm between the jaws and secondary grinding with an opening of approximately 5 mm. The grinding evolution is shown in Figure 2, Figure 3, and Figure 4.

Sieving classification

After the grinding beneficiation process, the fraction with the smallest grain size was separated using a sieve with an opening of 1.18 mm to delimit the appropriate diameter for the milling procedure in the following steps. The PG was dried at room temperature and the clods were manually separated until they all passed through a standard 1.18 mm sieve.

Figure 1 – **Flowchart of the experimental developed program**

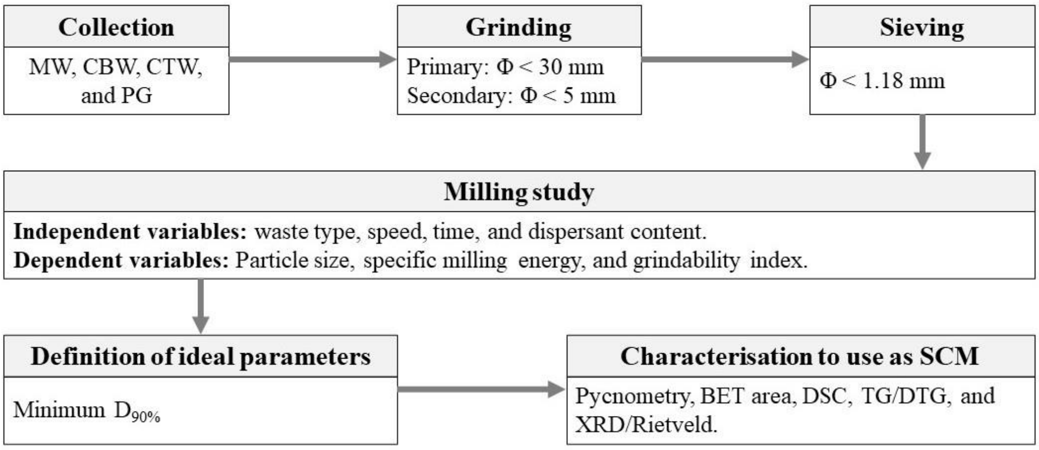

Figure 2 - **Marble waste grinding evolution – (a) material collected, (b) after primary grinding and (c) after secondary grinding**

Figure 3 – **Clay tile waste grinding evolution – (a) material collected, (b) after primary grinding and (c) after secondary grinding**

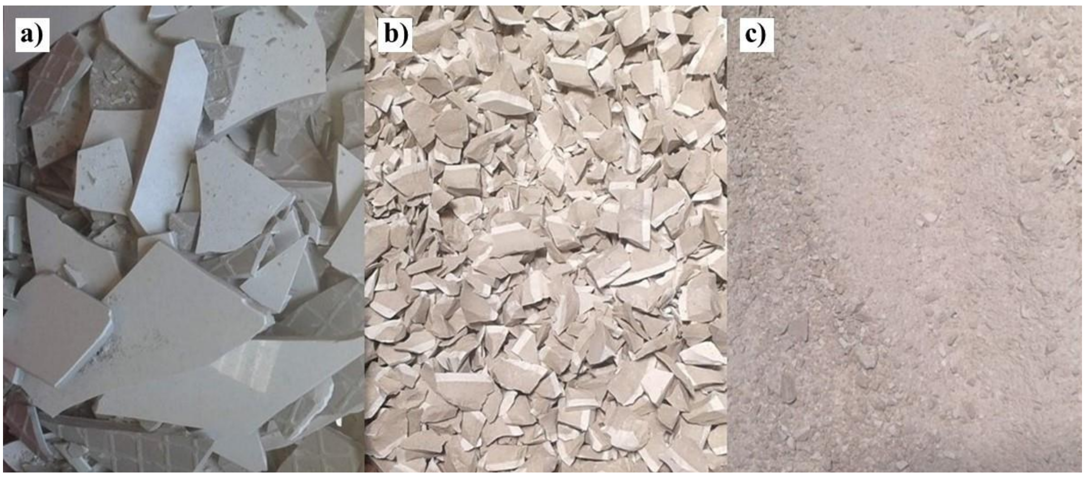

Figure 4 – **Clay brick waste grinding evolution – (a) material collected, (b) after primary grinding and (c) after secondary grinding**

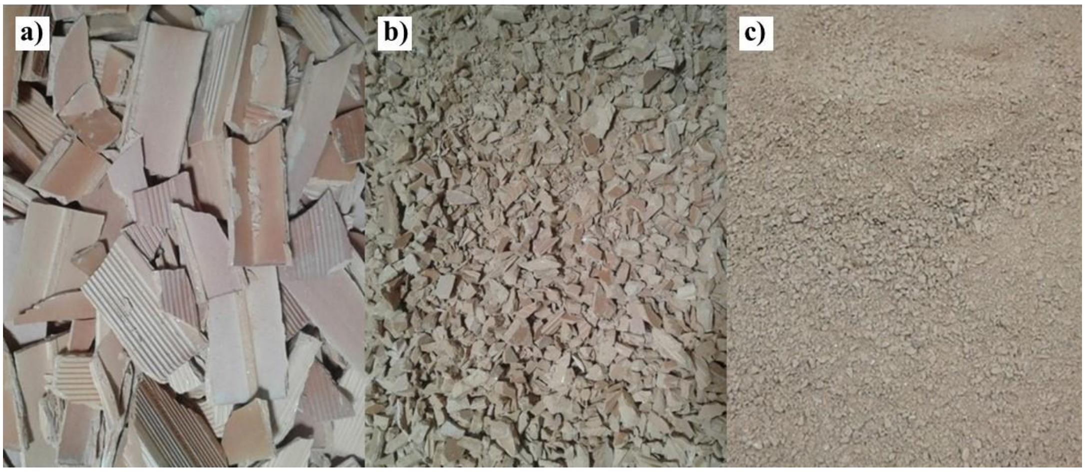

Milling study

The fractions of each material with particles smaller than 1.18 mm were subjected to the milling process in a PM 100 planetary ball mill (Retsch) equipped with a 500 cm^3 stainless steel milling jar. The materials were dried at 35 °C for 24 h in an oven before milling. The MW was milled under rotation speeds of 300 rpm and 400 rpm and the time was varied. The CBW and CTW were milled under 400 rpm and the time was varied. The PG was under 300 rpm and the processing time and dispersant content were varied. The milling jar was loaded with 1600 stainless steel balls (ϕ = 5 mm) and 210 g of CBW, 195 g of CTW, 208 g of MW or 183 g of PG, which correspond to mass ratios of spheres: powder of 3.8:1, 3.9:1, and 4.4:1, respectively. Propylene glycol was also added at a content of 0.2% as a dispersant to prevent agglomeration of the CBW and CTW on the spheres and against the inner faces of the milling jar. In the MW milling, 0.4% was applied. For PG, the content was varied between 0.2, 0.3, and 0.4% propylene glycol.

The granulometry of the waste after milling was evaluated by analysing the particle distribution by laser diffraction utilising a Mastersizer 3000 equipment (Malvern Instruments) equipped with an Aero S accessory for dry powder dispersion.

The specific milling energy was calculated as the ratio between the energy consumed during processing in the mill and the mass of material produced (KONG *et al*., 2013). The grindability index is associated with the potential to increase the specific surface area of a material during milling. This parameter was calculated by the ratio between the specific surface area and the energy consumed by the mill during processing (CASAGRANDE *et al*., 2017). The specific surface area for each milling scenario was estimated based on the particle distribution curve (DAMINELI *et al*., 2016).

Helium gas pycnometry

The waste specific mass was determined under optimal milling conditions and applying helium gas pycnometry, in the AccuPyc II 340 model device (Micromeritics).

Specific surface area (BET)

The specific surface area of the waste was determined by nitrogen physisorption isotherms at -196 °C using ASAP 2020 equipment (Micromeritics) and calculated by the Brunauer-Emmett-Teller (BET) method.

Differential scanning calorimetry

The specific heat of the waste was determined by a DSC-50 differential scanning calorimeter (Shimadzu). Samples of approximately 4 mg were placed in alumina crucibles and analysed under a nitrogen flow of 50 $mL.min^{-1}$. DSC measurements were performed in the temperature range between 25 °C and 150 °C. The schedule was initially set for a heating rate of 2 $°C.min^{-1}$ to 27 °C, followed by an isotherm for 10 minutes. A rate of 20 $°C.min^{-1}$ was then applied to 150 °C, and then the temperature was maintained for 30 min. The specific heat was calculated using the three curves, according to E 1269-11: standard test method for determining specific heat capacity by differential scanning calorimetry (AMERICAN..., 2018), in which aluminium oxide α was used as the specific heat reference.

Thermogravimetric analysis (TG/DTG)

Thermogravimetric analysis (TG) was performed on a DTG-60H thermal analyser (Shimadzu). About 10 mg of the powder samples were placed in alumina crucibles and analysed from 25 °C to 1000 °C, in synthetic air atmosphere (20% O_2, 80% N_2), with a flow rate of 50 $mL.min^{-1}$ and at a heating rate of 10 $°C.min^{-1}$.

X-ray diffractometry (XRD) and quantitative analysis by the Rietveld method

The XRD was applied to identify the mineralogical composition of the waste after the milling beneficiation process. The samples were analysed in a D8 Advance diffractometer (Bruker AXS) (radius of 280 mm) with Cu Kα radiation (λ = 0.154 nm) at 21 °C. Quantitative analysis was applied adopting the Rietveld method using the GSAS II software version 3913 (TOBY; VON DREELE, 2013), according to the methodology described by Costa *et al*. (2021).

Results and discussion

Optimisation of waste milling parameters

Marble waste

MW properties during and after milling are shown in Figure 5.

It can be observed that the energy consumption increases when the milling time is increased. The grindability index varies significantly as a function of time variation and, secondly, as a function of speed (Figure 6). This behaviour is inverse to that observed in marble milling done with a stirred media mill, in which speed is the determining parameter (TANER; TOROGLU, 2014).

Although the samples with the conditions of 20 min 300 rpm and 15 min 400rpm consumed the same energy in the processing, the first one reached smaller particle sizes. Thus, this was the condition chosen for evaluating the analysis stage of the potential use of MW as SCM.

Clay tile waste

The milling time was the main factor in reducing the CTW particle size (Figure 7).

The grindability index of CTW was significantly lower when compared to the other waste (Figure 8), due to the hardness of the material reached by the recrystallisation of the aluminosilicate clay minerals at the high firing temperatures during the clay tile production.

Figure 5 – **(a) Particle distribution and (b) cumulative frequency of the MW after milling**

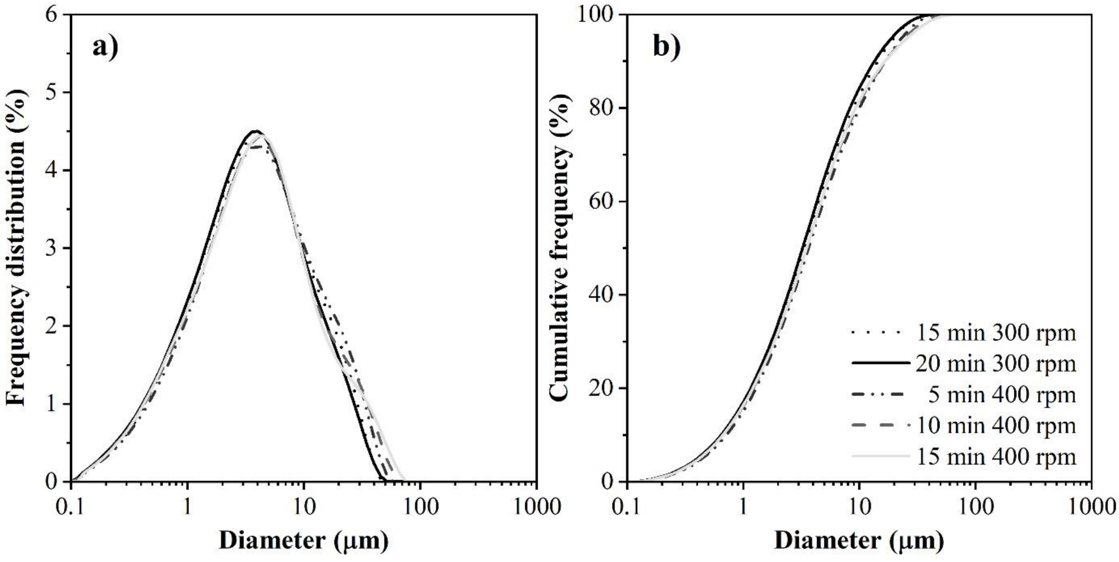

Figure 6 – **(a) D50%, (b) specific milling energy and (c) grindability index of MW after milling**

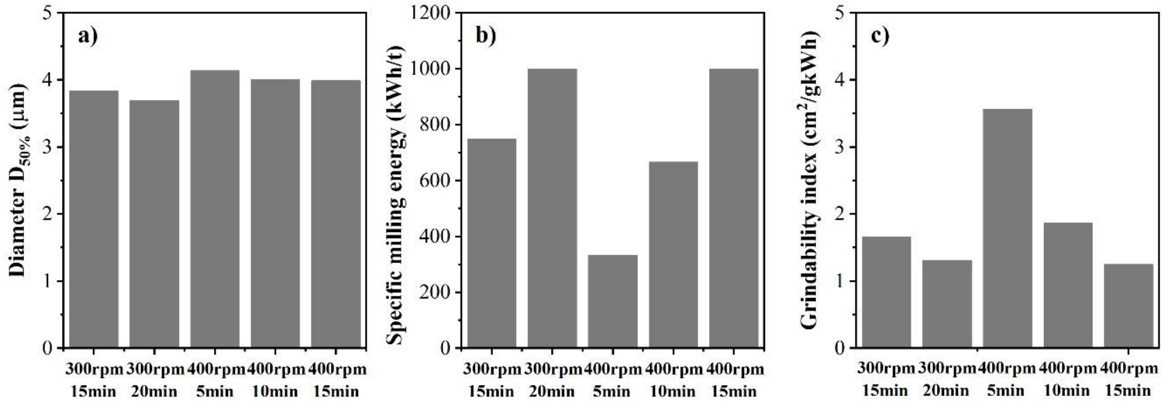

Figure 7 – **(a) Particle distribution and (b) cumulative frequency of the CTW after milling**

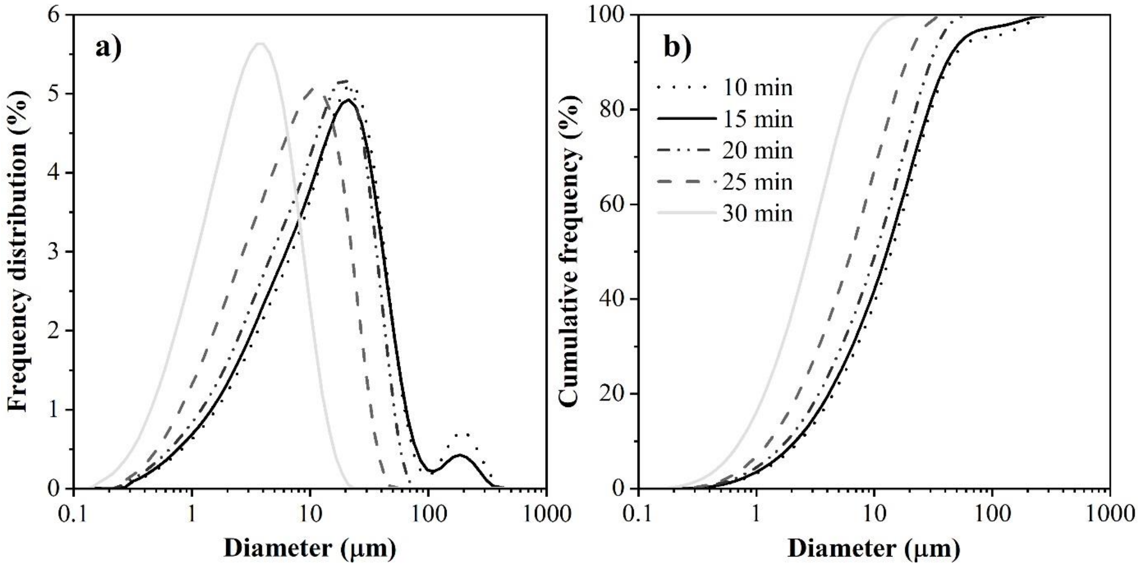

Figure 8 – **(a) D50%, (b) specific milling energy and (c) grindability index of the CTW after milling**

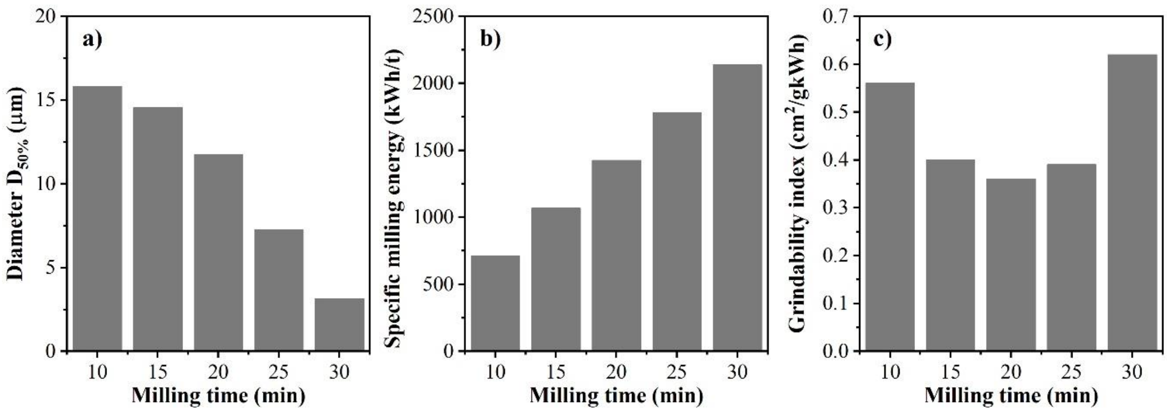

This behaviour indicates that CTW has high energy consumption while being processed, reducing its technical feasibility when compared to other calcined clay wastes. However, it should be considered that to reach $D_{50\%}$ similar to the 30 min sample (≈3 μm) with the same speed, previous studies required up to 2 hours of milling (ZHAO *et al*., 2020), even in scenarios where mills consumed twice as much energy (LIU *et al*., 2020). This demonstrates how the energy efficiency of the equipment used can influence the determination of the technical feasibility of processing a residual raw material. The condition chosen for the analysis of the potential use of CTW as SCM was 30 min at 400 rpm, aiming to maintain the diameter $D_{50\%}$ similar to MW and Portland cements (≈10 μm).

Clay brick waste

In CBW milling, time was the determining variable up to about 15 min (Figure 9). From this period onwards, the particle size tends to stabilise, leading to a slight variation in the diameter $D_{50\%}$. This effect is reflected in the milling index evolution, for which there is slight variation after 10 min, although the milling energy consumption increased (Figure 10).

The stabilisation level was only verified in the literature for times above 60 min applying the same speed (400 rpm) in a ball mill (ZHAO *et al*., 2020; LIU *et al*., 2020). This effect indicates the efficiency of the equipment model used, which, despite having consumed lower specific milling energies, led to a reduction in the particle size. Milling for 15 min compared to literature references reduced energy consumption by about 40% and shortened milling time by up to 105 min (ZHAO *et al*., 2020; LIU *et al*., 2020). The condition chosen to evaluate the potential use of CBW as SCM was 15 min at 400 rpm, aiming to reduce energy consumption in processing and ensuring a diameter $D_{50\%}$ similar to that of the CTW.

Phosphogypsum

Phosphogypsum milling was limited by the high tendency of the material to agglomerate. In scenarios with speeds or times greater than 300 rpm and 5 min, respectively, the waste adheres to the surfaces of the spheres and walls of the milling jar, becoming a solidified single piece. Therefore, these speed and time limits were fixed (Figure 11) and different levels of a dispersant additive (propylene glycol) were applied (Figure 12).

Figure 9 – **(a) Particle distribution and (b) cumulative frequency of CBW after milling**

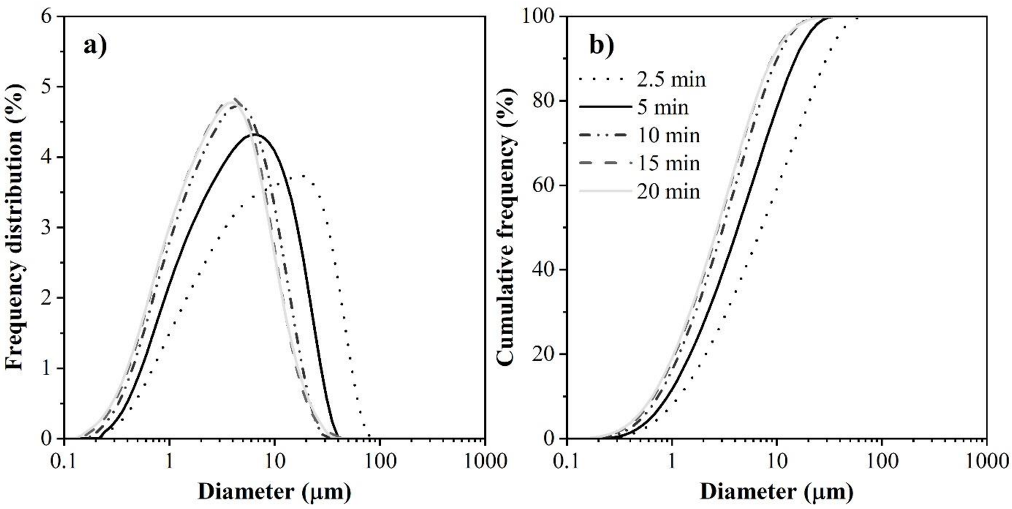

Figure 10 – **(a) Diameter D50%, (b) milling specific energy and (c) grindability index of the CBW after milling**

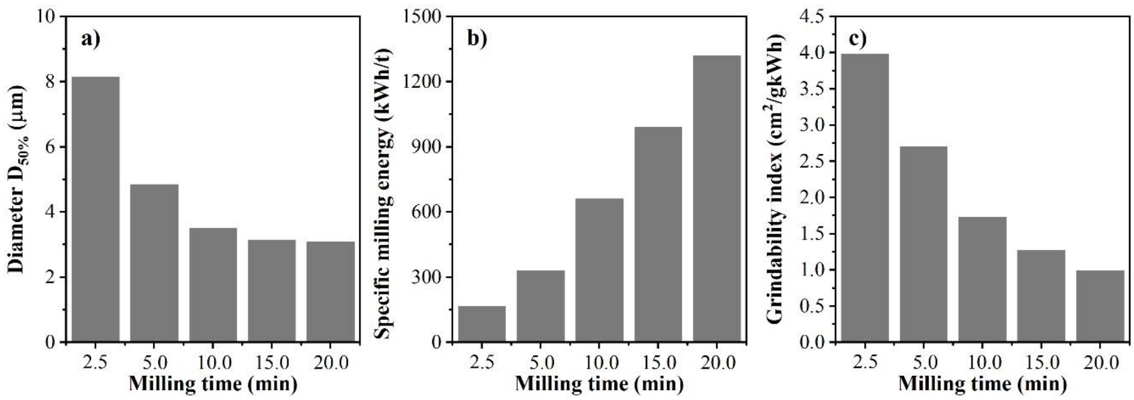

Figure 11 – **(a) Particle distribution and (b) cumulative frequency of PG after milling**

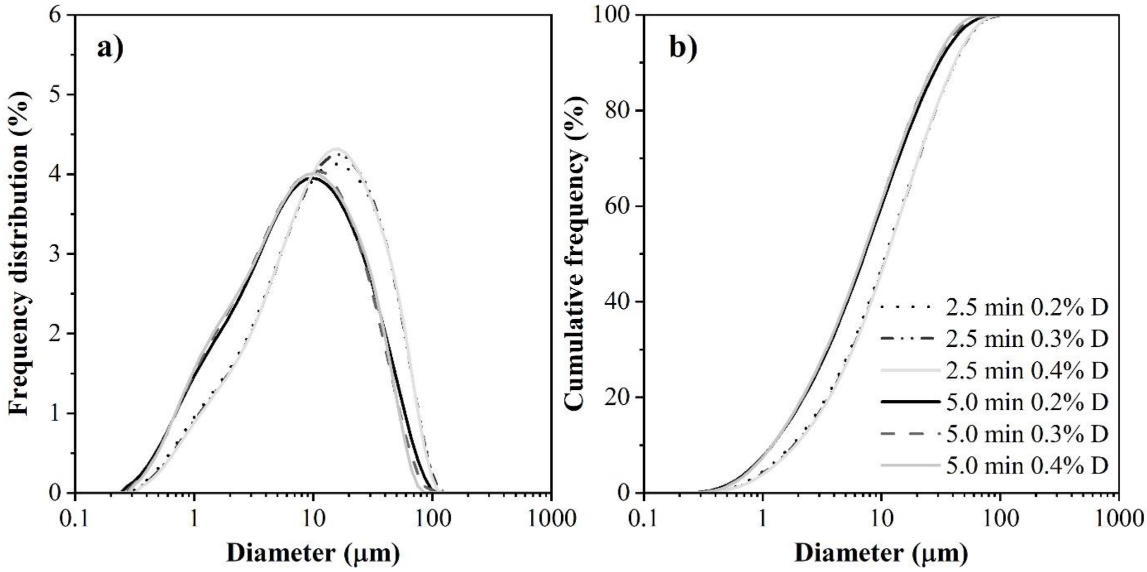

Figure 12 – **(a) Diameter $D_{50\%}$ and (b) grindability index of phosphogypsum after milling**

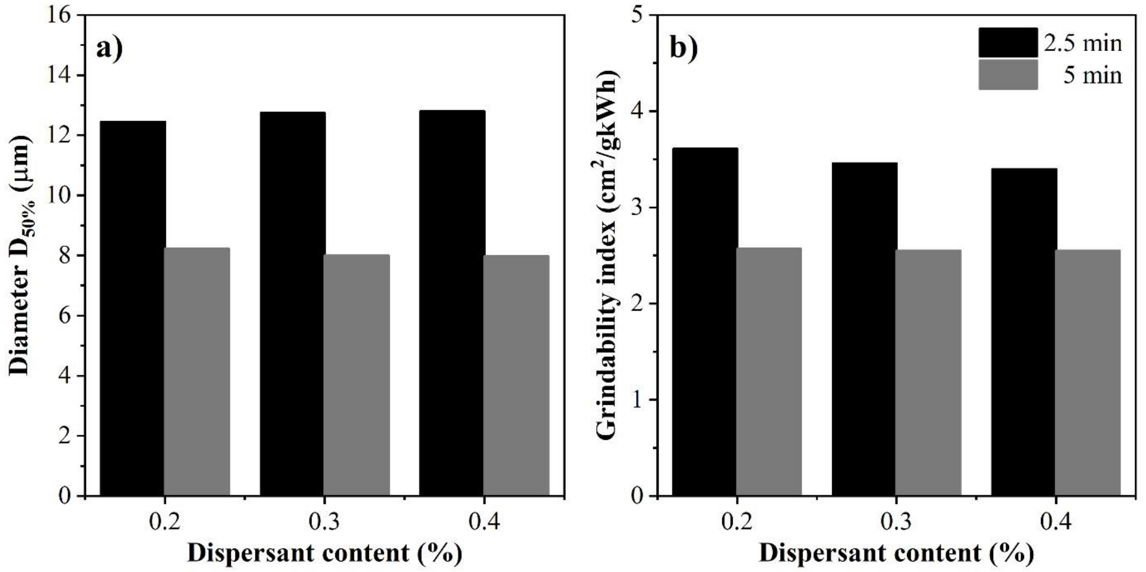

Only the samples submitted to 5 min of milling showed $D_{50\%}$ lower than that estimated for a conventional Portland cement (≈10 μm). Among these, the condition of 0.4% of dispersant was chosen for the analysis stage of the potential use of PG as SCM, as it presented the lowest $D_{90\%}$ (32.05 μm). Milling PG for 5 min promoted $D_{50\%}$ similar to what was found in the literature on milling gypsum for the same time (≈8 μm) (ÖKSÜZOĞLU; UÇURUM, 2016).

Analysing the potential for using waste as supplementary cementitious materials

Table 1 shows the physical properties of the waste after the milling process and considering the optimal conditions chosen in the previous step.

All waste reached similar or smaller particle sizes than those stipulated for conventional Portland cement, as well as high specific surface areas. NBR 16697: Portland cement: requirements (ABNT, 2018) defines cements containing mineral additions must have at least 88% of the particles with a diameter of less than 75 μm. Table 2 presents the chemical composition of the raw materials obtained by X-ray fluorescence spectrometry (XFS) using an S8 Tiger instrument (Bruker).

Table 1 - **Physical properties of waste after beneficiation**

Property	CBW	CTW	MW	PG
Specific mass (kg m^{-3})	2814	2601	2781	2438
BET specific surface area (m^2 kg^{-1})	9395	4540	9681	5119
Specific heat (J g^{-1} $°C^{-1}$)	1.10	0.83	1.25	1.08
D_{10} (µm)	0.77	0.83	0.73	1.37
D_{50} (µm)	3.14	3.14	3.69	7.98
D_{90} (µm)	10.20	8.61	15.33	32.05

The mineralogical composition of the raw materials was identified by TG/DTG and XRD/Rietveld (Figure 13). CBW has a loss on ignition of 1.09% in the range of 25 °C and 100 °C due to the free water loss. The mass consistency during the analysis up to 1000 °C indicates an efficient firing of the ceramic brick in the industry (MANOHARAN *et al.*, 2011; CLEGG *et al.*, 2012). This means that all clay minerals in the raw material reached the dehydroxylation temperature during firing. The same occurs for the CTW. PG has a mass loss of 20.03% in the temperature range of 100 °C and 190 °C due to the gypsum ($CaSO_4.2H_2O$) and brushite ($CaHPO_4.2H_2O$) dehydration temperature (LÓPEZ *et al.*, 2015; SCHOFIELD *et al.*, 2004). The MW shows a mass loss in the range of 500 °C to 800 °C attributed to the decarbonation of calcite ($CaCO_3$) and dolomite ($CaMg(CO_3)_2$) (RAMACHANDRAN *et al.*, 2002).

The diffractometric patterns of the waste are shown in Figure 14. The PG presents gypsum and brushite that were also identified in the TG results (Figure 15). CBW has a significant content of amorphous phases (75%). Clay firing at 850 °C causes dehydroxylation of clay minerals and promotes a structural disorder of the phases resulting in amorphous phases (SABIR *et al.*, 2001). Quartz is a material added by the ceramic industry to improve the thermal and dimensional stability of the ceramic brick (ARSENOVIC *et al.*, 2010).

XRD analysis determines the total SiO_2 content in the material, which is the percentage of oxides bound to different minerals, regardless of crystallinity. The XRD/Rietveld technique (with a correction for the non-crystalline phases content) allows the quantification of the crystalline phases of the material (WILL, 2006). Thus, the amount of SiO_2 bound to the crystalline phases can be determined through the stoichiometric analysis of the minerals in the crystalline fraction (SCRIVENER; SNELLINGS; LOTHENBACH, 2016). The difference between this value and the total SiO_2 content determined by XRD provides the silicon dioxide content in the material amorphous phase. In calcined clay materials, the amorphous part corresponds mainly to clay minerals after the dehydroxylation step (SABIR *et al.*, 2001). This effect occurs because the calcination of natural clay up to 850 °C causes the dehydroxylation of clay minerals, which promotes a structural disorder and results in the formation of non-crystalline phases (SABIR *et al.*, 2001). Calculating the SiO_2 and Al_2O_3 contents in the amorphous fraction of the sample makes it possible to identify the type of clay mineral constituting the natural clay of origin, which will influence the cementitious material properties combined with the calcined material (ZOLFAGHARNASAB; RAMEZANIANPOUR; BAHMAN-ZADEH, 2021). For CBW, for example, 64.78% of SiO_2 was detected by XRF and 22.35% of quartz was detected by XRD/Rietveld. In other words, the SiO_2 content in the clay mineral of this clay waste is 42.43%. As the Al_2O_3 content is 20.86%, a SiO_2/Al_2O_3 ratio of approximately 2.0 is identified, which is associated with the presence of montmorillonite (NASCIMENTO, 2016). For CTW, this proportion is 1.8, suggesting the presence of clay minerals in proportions of 1:1 (kaolinite) and 2:1 (montmorillonite) (NASCIMENTO, 2016).

MW has approximately 56% carbonates. Based on the decarbonation of calcite and dolomite, it can be estimated in the TG analysis that the mass losses of these phases are 20.87% and 4.03%, respectively. The difference between the estimated mass loss (24.90%) and the mass loss obtained by TG (41.49%) is due to the amorphous calcium carbonate not verified in XRD diffractograms. Considering that the amorphous content of WM (41.40%) is $CaCO_3$, the mass loss due to decarbonation would be 43.18%, which indicates that both techniques, TG and XRD, indicated similar results.

The degree of crystallinity is a fundamental factor for classifying ceramic waste (CBW and CTW) as SCM. Clay minerals in their raw form do not show pozzolanic activity. However, when they are calcined above the dehydroxylation temperature, there is an increase in the structural disorder, an increase in the reactivity of the material, and, consequently, the development of the pozzolanic potential (TEKLAY *et al.*, 2014). Therefore, the amorphous content reflects the pozzolanic reactivity of the CW as SCM. Calcined clays generally have a high content of non-crystalline phases (10 to 60%) (AVET *et al.*, 2018; HOLLANDERS *et al.*, 2016).

Table 2 - **Composition of waste oxides (%)**

Oxides (%)	CBW	CTW	MW	PG
SiO_2	64.78	65.02	4.53	1.09
Al_2O_3	20.86	20.23	0.45	0.11
Fe_2O_3	6.56	4.61	0.27	0.48
K_2O	3.43	2.16	0.07	49 ppm
MgO	1.29	0.98	3.7	0.02
TiO_2	0.94	0.51	0.03	0.68
Cr_2O_3	0.31	0.94	0.02	n. d.
Na_2O	0.12	3.06	n. d.	0.01
BaO	0.12	0.02	0.03	0.1
P_2O_5	0.11	0.06	0.01	0.73
CaO	0.09	1.29	49.03	33.02
NiO	0.09	0.24	0.01	19 ppm
SO_3	0.04	0.03	0.05	40.43
MnO	0.03	0.08	0.01	n. d.
V_2O_5	0.03	n. d.	n. d.	n. d.
SrO	0.02	0.01	0.02	0.56
CuO	0.02	0.03	34 ppm	n. d.
ZrO_2	0.02	0.62	20 ppm	0.03
ZnO	0.01	44 ppm	n. d.	n. d.
Rb_2O	0.01	0,01	n. d.	n. d.
Y_2O_3	0.01	41 ppm	n. d.	0.01
Ga_2O_3	35 ppm	22 ppm	n. d.	n. d.
As_2O_3	20 ppm	10 ppm	n. d.	n. d.
Nb_2O_5	17 ppm	7 ppm	n. d.	0.01
MoO_3	n. d.	n. d.	17 ppm	n. d.
CeO_2	n. d.	0.01	n. d.	0.21
La_2O_3	n. d.	n. d.	n. d.	0.09
Nd_2O_3	n. d.	n. d.	n. d.	0.07
HfO_2	n. d.	0.01	n. d.	n. d.
PbO	n. d.	41 ppm	n. d.	n. d.
LOI:	1.12	0.07	41.75	22.34

Note: LOI: Loss on ignition (1000 °C) determined by TG; n. d.: not detected; and ppm: parts per million.

Figure 13 - **Thermogravimetric analysis of waste materials**

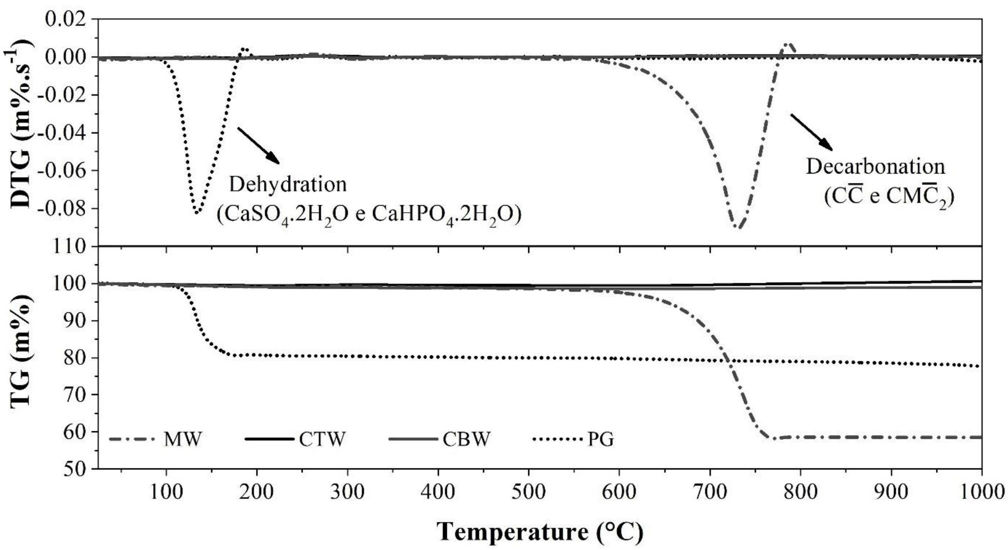

Figure 14 - **X-ray diffractometry of waste materials**

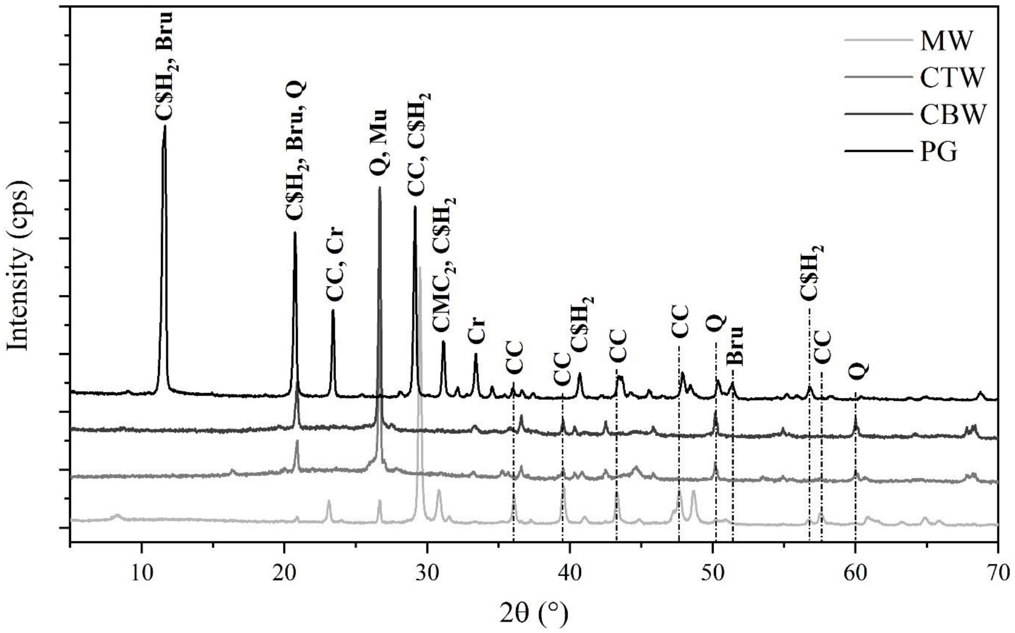

Figure 15 - **Mineralogical composition of waste obtained by XRD/Rietveld**

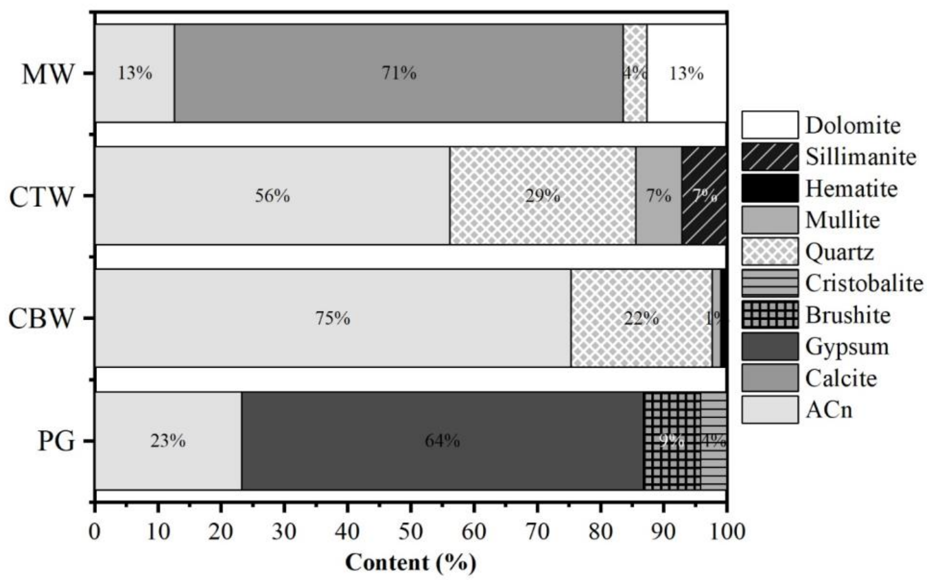

It is also observed that waste with mineralogical composition of phases formed at higher temperatures are associated with a higher demand for specific milling energy and lower grindability indexes. The CTW, for example, is the sample in which this effect was most expressive. The waste crystalline fraction essentially comprises mullite and sillimanite, which have formation temperatures of at least 1200 and 1400 °C, respectively, yielding higher binding energy and, therefore, greater hardness to the material.

According to the criteria of physical properties and mineralogical composition, the studied wastes have the potential for application as SCM. PG can be used as an alternative raw material to natural gypsum. CBW and CTW waste as an alternative to natural clays. The first is the most suitable due to the lower energy consumption for the milling process. Milled MW has the potential for use as an alternative to limestone filler in cementitious materials.

Conclusions

Based on the results, the following conclusions can be drawn:

(a) the grindability index is a determining factor in the optimisation of the milling parameters, allowing the evaluation of the particle size obtained for each condition, the degree of increase in the specific surface area, and the energy consumption during milling;

(b) the waste beneficiation in a high energy mill effectively reduced the particle sizes, reaching the proportions required for use as SCM;

(c) wastes with a mineralogical composition of phases formed at higher temperatures are associated with a greater demand for specific milling energy and lower grindability rates;

(d) beige Bahia marble waste has a mineralogical composition similar to that of commercial limestone and the physical properties can be achieved through milling;

(e) CTW and CBW have the potential for use as SCM to replace calcined natural clays, although CTW requires more energy during the milling process; and

(f) the analysed PG has the potential to be used as an alternative to natural gypsum in cementitious materials.

References

AMERICAN SOCIETY FOR TESTING AND MATERIALS. **E1269-11**: standard test method for determining specific heat capacity by differential scanning calorimetry. West Conshohocken, 2018.

ARSENOVIC, M. *et al*. Clay brick walls thermal properties. **International Journal of Modern Manufacturing Technologies**, v. 2, n. 1, p. 15-18, 2010.

ASSOCIAÇÃO BRASILEIRA DE NORMAS TÉCNICAS. **NBR 16697**: cimento Portland: requisitos. Rio de Janeiro, 2018.

AVET, F. *et al*. Determination of the amount of reacted metakaolin in calcined clay blends. **Cement and Concrete Research**, v. 106, p. 40-48, 2018.

AYDIN, E.; AREL, H. Ş. High-volume marble substitution in cement-paste: towards a better sustainability. **Journal of Cleaner Production**, v. 237, p. 117801, 2019.

CASAGRANDE, C. *et al*. Study of iron ore mixtures behavior in the grinding pelletizing process. **Mineral Processing and Extractive Metallurgy Review**, v. 38, n. 1, p. 30-35, 2017.

CHIODI FILHO, C. **O setor brasileiro de rochas ornamentais.** Rio de Janeiro: Associação Brasileira da Indústria de Rochas Ornamentais, 2018.

CLEGG, F. *et al*. Dehydroxylation and rehydroxylation mechanisms in fired clay ceramic: a TG-MS and DRIFTS investigation. **Journal of the American Ceramic Society,** v. 95, n. 1, p. 416-422, 2012.

CONNAN, H. *et al*. Thermal characterisation of autoclaved cement made with alumina-silica rich industrial waste. **Journal of Thermal Analysis and Calorimetry**, v. 84, n. 2, p. 521-525, 2006.

CONTRERAS, M. *et al*. Fractionation and fluxes of metals and radionuclides during the recycling process of phosphogypsum wastes applied to mineral CO_2 sequestration. **Waste Management**, v. 45, p. 412-419, 2015.

COSTA, A. R. D. *et al*. Hydration of sustainable ternary cements containing phosphogypsum. **Sustainable Materials and Technologies**, p. e00280, 2021.

DAMINELI, B. L. *et al*. Viscosity prediction of cement-filler suspensions using interference model: a route for binder efficiency enhancement. **Cement and Concrete Research**, v. 84, p. 8-19, 2016.

DEPARTAMENTO NACIONAL DE PRODUÇÃO MINERAL. **Sumário Mineral**. 2015. Available: http://www.anm.gov.br/dnpm/sumarios/sumario-mineral-2015. Access: Feb. 02, 2021

HOLLANDERS, S. *et al*. Pozzolanic reactivity of pure calcined clays. **Applied Clay Science**, v. 132, p. 552-560, 2016.

KABEER, K. S. A.; VYAS, A. K. Utilization of marble powder as fine aggregate in mortar mixes. **Construction and Building Materials**, v. 165, p. 321-332, 2018.

KONG, L. *et al*. Potential for reducing paper mill energy use and carbon dioxide emissions through plant-wide energy audits: a case study in China. **Applied Energy**, v. 102, p. 1334-1342, 2013.

LASSEUGUETTE, E. *et al*. Chemical, microstructural and mechanical properties of ceramic waste blended cementitious systems. **Journal of Cleaner Production**, v. 211, p. 1228-1238, 2019.

LAVAT, A. E. *et al*. Characterization of ceramic roof tile wastes as pozzolanic admixture. **Waste management**, v. 29, n. 5, p. 1666-1674, 2009.

LIU, Q. *et al*. Utilization potential of aerated concrete block powder and clay brick powder from C&D waste. **Construction and Building Materials**, v. 238, p. 117721, 2020.

LÓPEZ, F. A. *et al*. Thermal dehydration kinetics of phosphogypsum. **Materiales de Construcción**, v. 65, n. 319, p. 061, 2015.

MANOHARAN, C. *et al*. Analysis of temperature effect on ceramic brick production from alluvial deposits, Tamilnadu, India. **Applied clay science**, v. 54, n. 1, p. 20-25, 2011.

NASCIMENTO, G. M. **Clays, clay minerals and ceramic materials based on clay minerals**. Books on Demand, 2016.

ÖKSÜZOĞLU, B.; UÇURUM, M. An experimental study on the ultra-fine grinding of gypsum ore in a dry ball mill. **Powder Technology**, v. 291, p. 186-192, 2016.

PACHECO-TORGAL, F.; JALALI, S. Reusing ceramic wastes in concrete. **Construction and Building Materials**, v. 24, n. 5, p. 832-838, 2010.

RAMACHANDRAN, V. S. *et al*. **Handbook of thermal analysis of construction materials**. New York: Noyes Publications, William Andrew Publishing, 2002.

RASHAD, A. M. Phosphogypsum as a construction material. **Journal of Cleaner Production**, v. 166, p732-743, 2017.

ROBAYO-SALAZAR, R. A. *et al*. Eco-efficient alkali-activated cement based on red clay brick wastes suitable for the manufacturing of building materials. **Journal of Cleaner Production**, v. 166, p. 242-252, 2017.

SABIR, B. B. *et al*. Metakaolin and calcined clays as pozzolans for concrete: a review. **Cement and concrete composites**, v. 23, n. 6, p. 441-454, 2001.

SCHOFIELD, P. F. *et al*. The role of hydrogen bonding in the thermal expansion and dehydration of brushite, di-calcium phosphate dihydrate. **Physics and Chemistry of Minerals**, v. 31, n. 9, p. 606-624, 2004.

SCRIVENER, K.; SNELLINGS, R.; LOTHENBACH, B. (dd.). **A practical guide to microstructural analysis of cementitious materials**. Boca Raton: CRC Press, 2016.

SHAO, J. *et al*. Study on the pozzolanic reaction of clay brick powder in blended cement pastes. **Construction and Building Materials**, v. 213, p. 209-215, 2019.

SHEN, W. *et al*. Utilization of solidified phosphogypsum as Portland cement retarder. **Journal of Material Cycles and Waste Management**, v. 14, n. 3, p. 228-233, 2012.

TANER, H. A.; TOROGLU, I. Effect of operational parameters on the particle size distribution of marble wastes in stirred media mill. In: MINE planning and equipment selection. Cham: Springer, 2014.

TEKLAY, A. *et al*. Calcination of kaolinite clay particles for cement production: a modeling study. **Cement and Concrete Research**, v. 61, p. 11-19, 2014.

TOBY, B. H.; VON DREELE, R. B. GSAS-II: the genesis of a modern open-source all purpose crystallography software package. **Journal of Applied Crystallography**, v. 46, n. 2, p. 544-549, 2013.

TOLEDO FILHO, R. D. *et al*. Potential for use of crushed waste calcined-clay brick as a supplementary cementitious material in Brazil. **Cement and Concrete Research**, v. 37, n. 9, p. 1357-1365, 2007.

UYGUNOĞLU, T. *et al*. Use of waste marble and recycled aggregates in self-compacting concrete for environmental sustainability. **Journal of Cleaner Production**, v. 84, p. 691-700, 2014.

VARDHAN, K. *et al*. Mechanical properties and microstructural analysis of cement mortar incorporating marble powder as partial replacement of cement. **Construction and Building Materials**, v. 96, p. 615-621, 2015.

WILL, G. **Powder diffraction**: the Rietveld method and the two-stage method to determine and refine crystal structures from powder diffraction data. Heidelberg: Springer Science & Business Media, 2006.

ZHAO, Y. *et al*. The particle-size effect of waste clay brick powder on its pozzolanic activity and properties of blended cement. **Journal of Cleaner Production**, v. 242, p. 118521, 2020.

ZOLFAGHARNASAB, A.; RAMEZANIANPOUR, A. A.; BAHMAN-ZADEH, F. Investigating the potential of low-grade calcined clays to produce durable LC^3 binders against chloride ions attack. **Construction and Building Materials**, v. 303, p. 124541, 2021.

Ana Rita Damasceno Costa
Programa de Pós-Graduação em Engenharia Civil, Escola Politécnica | Universidade Federal da Bahia | Rua Professor Aristides Novis, 02, Federação | Salvador – BA – Brasil | CEP 40210-630 | E-mail: rita.damasceno@ufba.br

Jardel Pereira Gonçalves
Centro Interdisciplinar de Energia e Ambiente, Escola Politécnica | Universidade Federal da Bahia | Tel.: (71) 3283 9485 | E-mail: jardelpg@ufba.br

Ambiente Construído
Revista da Associação Nacional de Tecnologia do Ambiente Construído
Av. Osvaldo Aranha, 99 - 3º andar, Centro
Porto Alegre – RS - Brasil
CEP 90035-190
Telefone: +55 (51) 3308-4084
www.seer.ufrgs.br/ambienteconstruido
www.scielo.br/ac
E-mail: ambienteconstruido@ufrgs.br